Journal of Computers Vol. 32 No. 3, 2021, pp. 99-118
doi:10.3966/199115992021063203008

Hierarchical Linear Model Approach to Explore Interaction Effects of Swimmers' Characteristics and Breathing Patterns on Swimming Performance in Butterfly Stroke with Self-Developed Inertial Measurement Unit

Cheng-Chang Jeng*

Department of Education, National Taitung University, Taitung 950, Taiwan, ROC
jengcc@gmail.com

Received 29 August 2020; Revised 12 January 2021; Accepted 24 February 2021

Abstract. An inertial measurement unit (IMU) was developed by programming in an Arduino environment to obtain breathing motion data from nine semi-professional swimmers in a university swimming team while they swam four 50m laps using the butterfly stroke. The results indicated that the proposed device can help coaches and researchers distinguish breathing and non-breathing processes and effectively read the pitch angle and time information of breathing motions during the butterfly stroke. Furthermore, a hierarchical linear model (HLM) approach was employed to examine the interaction effects of the individual variables of the swimmers and their breathing patterns on their swimming efficiency. This analysis showed that significant interaction effects exist between age and average breathing time, significantly influencing swimming efficiency. It also indicated that significant interaction effects exist between gender and the number of breaths taken and between gender and average maximum breathing angle. Lastly, significant interaction effects exist between the body mass index (BMI) of the swimmers and the number of breaths taken and between BMI and average maximum breathing angle. These results demonstrate the efficacy of the proposed IMU, which could be effectively applied to help coaches and researchers analyze and enhance swimmers' performance.

Keywords: hierarchical linear model, Arduino, inertial measurement unit, butterfly stroke, breathing patterns

1 Introduction

In this section, posture factors and swimmers' individual variables that may affect performance of butterfly strokes are presented. After that, the two methods for acquiring swimming posture data, using video-based equipment and IMU, are shown. Research motivation and purpose are finally introduced at the end of this section.

1.1 Posture Factors Affecting Swimming Performance in Butterfly Strokes

Phelps, Bowman, and Hoff [1] suggested that during swimming, the head and the torso should form a straight line to reduce drag. This forms the primary focus in the evaluation of a swimmer's posture. The roll angle of the body when the swimmer takes a breath is also greater than that when the swimmer is not taking a breath, which causes the body to lose its streamlined shape and increases drag. Cortesi and Gatta [2] observed 10.4~10.9% less passive drag when the head is down and below the outstretched arms than when the head is up. Thus, smaller pitch and roll angles of the head will yield greater swimming efficiency. Reducing breathing frequency can also increase swimming efficiency but reduces the oxygen supply and increases the CO_2 concentrations in the body. This is one of the main causes of swimmer

* Corresponding Author

fatigue [3]. Overall, breathing affects the streamlined shape of the body, thereby increasing drag and reducing swimming speed. Thus, aside from the angle of breathing, the number of breaths taken is also a crucial factor influencing swimming performance.

The butterfly is a swimming stroke that requires endurance and skill. A single butterfly stroke can be divided into four phases: the beginning of the cycle (i.e., start position), pre-thrust, thrust, and gliding (i.e., recovery). These are depicted in Fig. 1. It is during the thrust phase that the greatest drag appears; this is when the swimmer takes a breath.

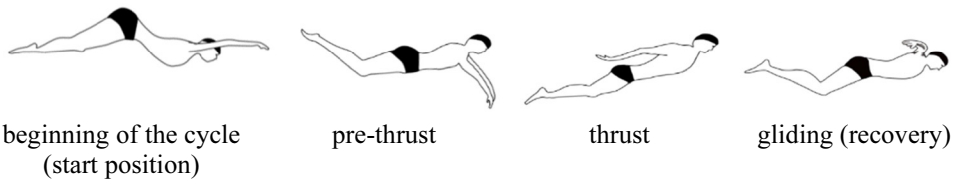

Fig. 1. Phases of butterfly stroke

Staniak et al. [4] fixed a factory made IMU on the dorsal portion of the pelvic girdle of a swimmer to investigate the body motion in butterfly swimming. Their study confirmed that body coordination in phases of butterfly strokes and prevention of dramatic velocity change may improve swimming economy and average swimming velocity. Similarly, Gonjo and Olstad's study [5] also revealed that butterfly swimmers should avoid dramatic changes of body angles so as to reduce swimming drag. Cortesi and Gatta [2] indicated that the posture of hiding the head below the outstretched arms corresponds to the start position of the butterfly stroke, so it makes sense that the drag is lowest at the start position. The drag is highest during the thrust phase, so during the subsequent recovery phase, the swimming speed is much slower. Taiar et al. [6] conducted a fluid dynamics experiment on the individual postures in the butterfly-stroke phases using a mannequin in a flume and discovered that the drag coefficient of the posture was the highest at the end of the thrust cycle and lowest at the beginning of the cycle. Thus, it is clear that drag is the greatest during and after breathing. The studies above indicate that the frequency and angle of breathing influence swimming efficiency; however, few studies have examined the connection between these variables and swimming efficiency for the butterfly stroke.

1.2 Individual Variables Affecting Swimming Performance

Aside from the factors related to swimming posture, the individual variables of the swimmer, such as gender, age, height, and weight, are also crucial factors influencing performance. Most race athletes are at their peak from adolescence to around the age of 30; this includes swimming athletes.

Vaso et al. [7] observed that among elite Swiss swimmers, men and women achieved their peak swimming speed at around 22-25 and 20-21 years old, respectively. After that, their swimming speed declined with age. Gender is also a factor that influences swimming performance. In most race competitions, female athletes are not as fast as male athletes. In swimming, the swimming speeds of male and female swimmers present a greater difference. However, as the distance increases, such as in a 1,500-meter race, the difference between the lap times of male and female swimmers becomes smaller [8]. Furthermore, the height and weight of the swimmer are also crucial factors affecting swimming performance. Sedeaud et al. [9] discovered that the body mass index (BMI), calculated as kilograms per meter squared, is an important index for the analysis of swimmer performance. Their results revealed that short-distance swimming athletes have higher BMI values than long-distance swimming athletes, mainly because short-distance races involve greater oxygen consumption and muscle power, which favor taller and heavier physiques. In contrast, long-distance swimmers tend to have smaller and lighter physiques. Although there are many factors that influence swimming performance, the interaction effects among individual variables and posture factors on swimming efficiency have rarely been examined in previous studies.

1.3 Analyzing Swimming Posture Data Using Video-based Approaches

To obtain swimming posture data, most studies use video filming to analyze swimming motions. Researchers have pointed out that approximately 3/4 of coaches use filming to analyze the motions of

elite swimmers and help swimming athletes improve their skill [10]. The captured video segments must be input to a computer for post-processing and analysis [11-12]; this is time-consuming and cannot immediately provide swimmers with feedback to improve their motor skills. Furthermore, capturing motions underwater requires at least one piece of underwater filming equipment, and tracking the motions of the swimmer during each lap requires an underwater rail camera. Although underwater cameras are effective at capturing underwater motion, their installation costs are high, which means they are rarely installed in venues not designed for professional training [13].

Installing underwater cameras and rails entails a complicated experimental setup. It is costly in terms of both time and money and is therefore only done in swimming training institutions dedicated to training elite swimmers. Moreover, swimmers' performance in experimental scenarios is likely different from their performance in natural circumstances [14]. Overall, using video filming equipment to analyze swimming motions is limited by the following [15-18]: (1) long installation time and expensive installation environments and equipment, (2) long video processing time, (3) water flow disturbances, light reflected off water surfaces, and foam in the aquatic environment affecting video capture and interpretation, and (4) parallax preventing capture of motion details.

1.4 Analyzing Swimming Posture Data Using Inertial Measurement Units

Advances in electronic technology and sensor miniaturization in recent years now enable sensors to be directly worn by athletes to record their motions and responses, which overcomes the shortcomings of video-based swimming analysis systems. These sensors, which include accelerometers, gyroscopes, and magnetometers, are referred to as inertial measurement units (IMUs). A single IMU may contain one to all three of these sensing elements. In past research, IMUs have proven powerful tools for swimmer posture analysis, and they are not limited to certain experiment venues or laboratories. IMUs can be used to obtain measurements in natural swimming environments, which means they can gather more swimming data than most video-based experiment environments [19].

Most of the existing studies that used IMUs to analyze swimming motions installed the sensors on the upper limbs [18] or wrists [20] to analyze hand motions; few have examined head motions and breathing patterns. Pansiot et al. [16] analyzed wearable locations for IMUs and observed that devices worn on the torso or head are suitable for the four primary swimming styles (front crawl, backstroke, breaststroke, and butterfly). They also determined that these locations are best for obtaining data regarding overall motions. They modified an ear-worn activity-recognition sensor and fastened it to the left rubber strap of the swimmer's swimming goggles to analyze the pitch and roll angles of the head. The data was stored in a built-in memory and then transmitted wirelessly to a computer after the experiment for processing. One of the further benefits of this type of device worn in this way is that there is less interference with the motions of the swimmer [18].

Most studies introduced in this subsection applied commercial IMUs to acquire motion data of swimming [16-18, 20], which limits researchers to the use of closed software and hardware. As a consequence, researchers are unable to modify devices or software coding to meet research needs and lower research expenses. For example, Pansiot et al.'s commercial IMU [16] worked with a closed platform environment which only enables analysis using dedicated software. Also, Staniak et al. [4] applied a commercial IMU placed on the torso to analyze movements in butterfly strokes. If researchers were to adopt Staniak et al.'s IMU to analyze butterfly-stroke head movements, the software coding and algorithms would need to be modified to collect substantially distinct motion data from different body locations. Thus, there is a need to develop a small, lightweight IMU that operates in an open-source software environment.

1.5 Research Motivation and Purposes

The studies described in previous sections obtained robust findings regarding the influence of biological factors, breathing angles, and breathing frequency on swimming efficiency. However, the majority of these studies used more expensive and difficult-to-install cameras to obtain swimming movement data. The butterfly stroke creates more foam, which affects image interpretation, and during the butterfly stroke, the head and the torso emerge from the water but then immediately re-submerge. With a conventional setup, cameras are required to film in and out of the water simultaneously because if underwater cameras are used exclusively, then the full range of butterfly stroke motions cannot be

captured. Such technology is expensive, which is why few studies have investigated the influence of breathing patterns on butterfly-stroke swimming efficiency.

This study aimed to reduce the costs of swimming data acquisition and shorten data-processing time. After that, the data will be analyzed to investigate the relationships among individual variables, breathing patterns, and swimming efficiency. Thus, our objectives were as follows: (1) use open software and hardware to develop a low-cost, portable IMU for swimming movement research, (2) conduct this study in a real-world scenario, and (3) use the developed IMU to analyze the influence of interaction effects among swimmers' characteristics and breathing patterns on butterfly-stroke swimming efficiency.

2 Method

This section describes the hardware and firmware design in an Arduino development environment and explains butterfly-stroke data acquisition with the proposed device as well as post-processing.

2.1 Hardware

Most of the studies employed commercially-available IMU products that come with closed-format. This induces greater costs, and in raw data acquisition, only the formats provided by the manufacturer are available. Thus the Arduino development environment with open software and hardware was adopted to design an IMU that can measure the head posture of swimmers. As shown in Fig. 2, the hardware framework comprises two parts. The dotted box on the left shows the charging and power supply circuits; the dotted box on the right presents the MCU and IMU data storage circuits. The J5019 module charges a Li-ion battery via USB and increases the voltage of a 3.7-V 1400-mAh Li-ion battery to supply power to the other electronic modules. The J5019 module also increases the voltage of a 3.7-V 1400-mAh Li-ion battery from 5 V to 9 V to provide power to Arduino Nano. The MPU6050 transmits real-time IMU data to Arduino Nano via I2C protocol, then Arduino Nano stores data to a Micro SD card via SPI protocol. A USB card reader then reads the motion data recorded in the SD card and transmits it to the computer for post-processing.

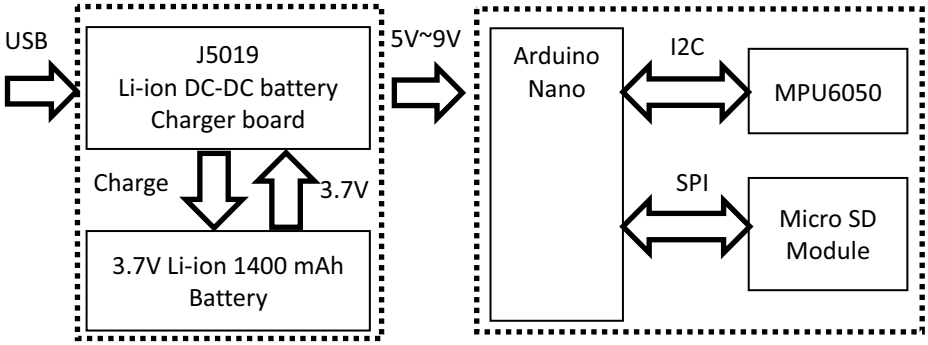

Fig. 2. Hardware framework

The left image in Fig. 3 presents the modules. Each square on the green grid beneath the modules is 1cm×1cm; these green grids indicate the dimensions of the modules. The circled numbers in the images mark the following components: (1) 3.7-V Li-ion battery, (2) Arduino Nano, (3) J5019 charging/step-up dual-purpose module, (4) micro SD data storage module, and (5) MPU6050 module. The right image in Fig. 3 presents the wired and assembled product with the dimensions of 48mm×55mm×15mm and mass of 50.3 g. Because it would be used in an aquatic environment, a waterproof liquid silicone rubber (LSR) coating was added to protect the electronic components and the modules and wires were fixed using hot glue.

Fig. 3. Component modules (left) and finished product (right)

2.2 Firmware

Before developing the IMU, a calibration program developed by Luis Ródenas [21] was burned into Arduino Nano to record the offset values from the MPU6050 module. Placing the IMU horizontally, 1,100 items of raw data were read from the accelerometer and the last 1,000 items were averaged as the offset values. The serial monitor of the Arduino IDE displayed the offset values of the three axes, and these offset values were recorded to correct any errors in the MPU6050.

In order to develop the firmware to read pitch and roll angles, the MPU6050 procedure, getMotion6, was used to obtain raw three-axis data from the accelerometer at a sample rate of 50 Hz, from which the previously obtained offsets were subtracted. Then, Eqs. (1) and (2) were employed to convert the data into pitch and roll angles, respectively [22]. The radian units [-π/2, π/2] were then mapped to degree units [-90°, 90°]:

$$\text{Pitch} = \arctan\left[\frac{A_x}{\sqrt{(A_y)^2+(A_z)^2}}\right]\times\frac{180°}{\pi}. \tag{1}$$

$$\text{Roll} = \arctan\left[\frac{A_y}{\sqrt{(A_x)^2+(A_z)^2}}\right]\times\frac{180°}{\pi}. \tag{2}$$

In Eqs. (1) and (2), Ax, Ay, and Az respectively denote the acceleration values in the directions of the X, Y, and Z axes. The firmware was written using Arduino IDE and then burned into the Arduino Nano. Fully charged, the device was set to store an item of IMU data every 20 ms (i.e., 50 items of data per second) and work continuously for 4 hours or more. Using these settings, the Arduino algorithm was as shown in Algorithm 1.

Algorithm 1. Arduino algorithm for detecting pitch-and-roll angles

Line	Statement
1	`include module supportive files;`
2	`initialize Variables; Set samplingInterval = 20 ms;`
3	`MPU6050 accelgyro; //Declare MPU6050 Object`
4	`void setup() {`
5	`  initialize Serial Port, SD module, and MPU6050 Module;`
6	`  Stop this program if failed to initialize;`
7	`  prepare SD card for data writing;`
8	`  accelgyro.setXAccelOffset(469.6236);`
9	`  accelgyro.setYAccelOffset(-591.6900);`
10	`  accelgyro.setZAccelOffset(-1156.14);`
11	`} //end of setup()`
12	`void loop() {`
13	`  if (currentTime - previousTime >= samplingInterval)`
14	`  {`

```
15            previousTime = currentTime;
16            accelgyro.getMotion6(&ax, &ay, &az, &gx, &gy, &gz);
17            float pitch = atan(ax/sqrt(ay*ay+az*az))*180.0/PI;
18            float roll = atan(ay/sqrt(ax*ax+az*az))*180.0/PI;
19            write accelerator raw data to SD card;
20            write pitch angle and roll angle to SD card;
21      } //end of if
22  } //end of loop()
```

In Algorithm 1, Lines 1~2 initialize the library needed by the sensor module and the variables used in the program. Line 3 declares the instance of MPU6050 for the main program loop() to use. Lines 4~11 present the Arduino setup() function, which is used to set up variables, use libraries, and initialize hardware modules. Lines 4~7 first set the SD card, and then Lines 8~10 set the offset values of the MPU6050. Lines 12~22 are the main program, among which Lines 13~15 indicate that after each sampling interval, Lines 16~18 initiate reading of the IMU data and convert the data into pitch and roll angles. Finally, Lines 19~20 write the raw data and the angle data into the SD card.

2.3 Data Acquisition and Processing

The developed device was kept in a waterproof ziplock bag, as shown on the left of Fig. 4, and then placed inside the swimming cap of the swimmer. Using the swimmer's goggle straps, it was fixed so that it would stay roughly as high as the upper edges of the ears. Using a right-angle ruler, it can be confirmed that the IMU was at a 90-degree angle to the water surface when the swimmer stood upright, as shown on the right of Fig. 9. The bright spot in the picture is an LED light that helped us confirm the operating conditions of the IMU.

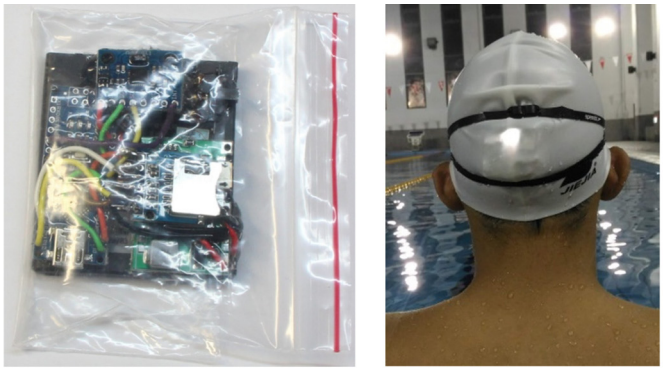

Fig. 4. Device in waterproof ziplock bag (left) and under swimming cap and goggle straps (right)

The participants of this study were 4 female and 5 male volunteers and their willingness to participate was confirmed through written consent. The research objectives, the features of our equipment, and documents for the experiment proposal were explained to all of the participants. On the day of the experiment, we verbally explained the content and process of the experiment to the participants again. The participants were also reminded that the experiment could be aborted at any time if they were in any physical discomfort. The experiment venue was at a university swimming pool. Two lifeguards and one assistant were present during the experiment. All of the nine participants were members of the university swimming team, had competed in national swimming races before, and had earned lifeguard certificates. Thus, they were semi-professional swimmers. The average height, weight, and age of the female swimmers were 167.2 cm, 59.6 kg, and 20.8 years old, and the average height, weight, and age of the male swimmers were 176.6 cm, 74.8 kg, and 21.4 years old.

Only one swimmer was measured at a time. In the 25m-long pool, they first did a warm-up by swimming 100 meters using front-crawl swimming. Then, using what they felt was their normal swimming speed during practice, they swam four 50m laps using the butterfly stroke. Between laps, the swimmers were asked to rest until they felt that their heart rate had recovered and that they could continue with the experiment. The purpose of this was to enable the swimmers to swim using their normal and natural swimming postures rather than fatigued swimming postures. During the experiment,

the assistant followed the swimmers and filmed them using a handheld camera. After they completed the four 50m laps using the butterfly stroke, the IMU was retrieved and the data in the SD were downloaded to a computer for data processing. Fig. 5 presents the data of pitch and roll angles obtained from the fourth lap of a swimmer. The solid blue line shows the pitch angles of the head calculated using Eq. (1), whereas the dashed red line shows the roll angles calculated using Eq. (2).

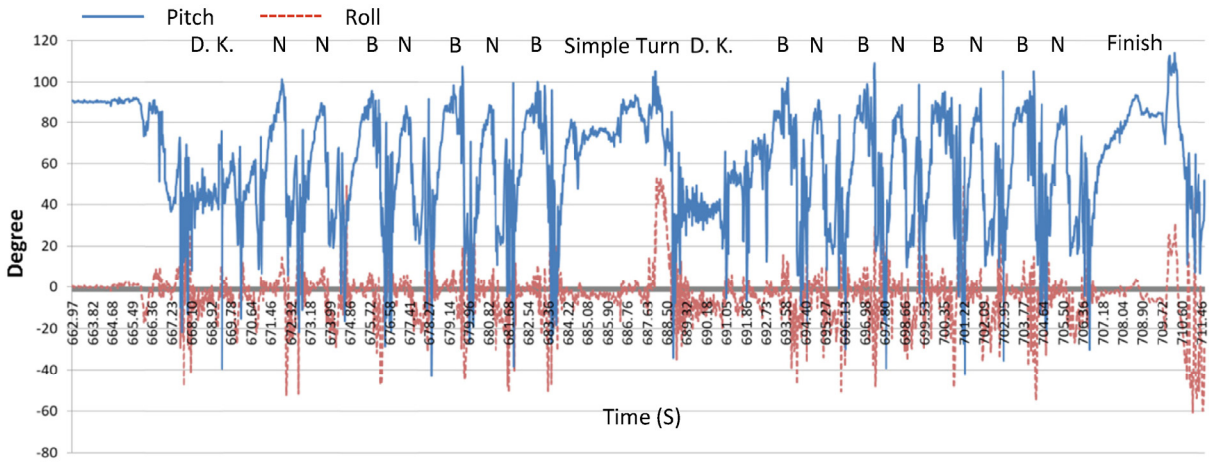

Fig. 5. Pitch-and-roll angle data of swimmer's head obtained by IMU during butterfly stroke

In Fig. 5, B marks the breathing motions; N indicates the non-breathing motions, and D. K. indicates when dolphin kicks were made. As can be seen, the duration of a breathing motion is longer than that of a non-breathing motion, and the pitch angle of the head is greater during a breathing motion than during a non-breathing motion. It is evident from this representation that IMUs are a simple and convenient way of observing breathing and non-breathing motions during the butterfly stroke.

3 Results

This section presents the connection between IMU data and different stages of the butterfly stroke to explain the importance of conducting a statistical interaction analysis. Using HLM software [23], the interaction effects of the individual variables of swimmers and breathing motion data on swimming performance was analyzed.

3.1 Analysis of Butterfly Stroke and Breathing Motions Using IMU Data

Fig. 6 enlarges the section between 674.86 seconds and 679.96 seconds in Fig. 5. This makes the details of the angle changes clearer, which makes it easy to associate these with various stages of the butterfly stroke. In Fig. 6, D. K. indicates a dolphin kick. Between 674.81 seconds and 675.29 seconds is the accelerating thrust of Motion T. At around 675.78 seconds, the pitch angle of the head is the greatest. This is during Motion B when the arms are lifted above and behind, and the swimmer finishes taking a breath. This is immediately followed by the gliding and recovery of Motion R. Next, the head swiftly faces the bottom of the pool, and the pitch angle drops. This is Motion S, which completes the breathing motion and resets to the start position. Furthermore, the period marked as the "thrust and breathing time" in Fig. 5 is the period when the butterfly stroke accelerates and breathing is completed, which is referred to simply as the breathing motion in this study. From the period between 676.68 seconds and 677.50 seconds, it depicts that the breathing motion takes more time than the non-breathing motion and that the maximum pitch angle during the breathing motion is also greater than that during the non-breathing motion. Thus, it can be seen that using an IMU to analyze butterfly stroke movements has practical value.

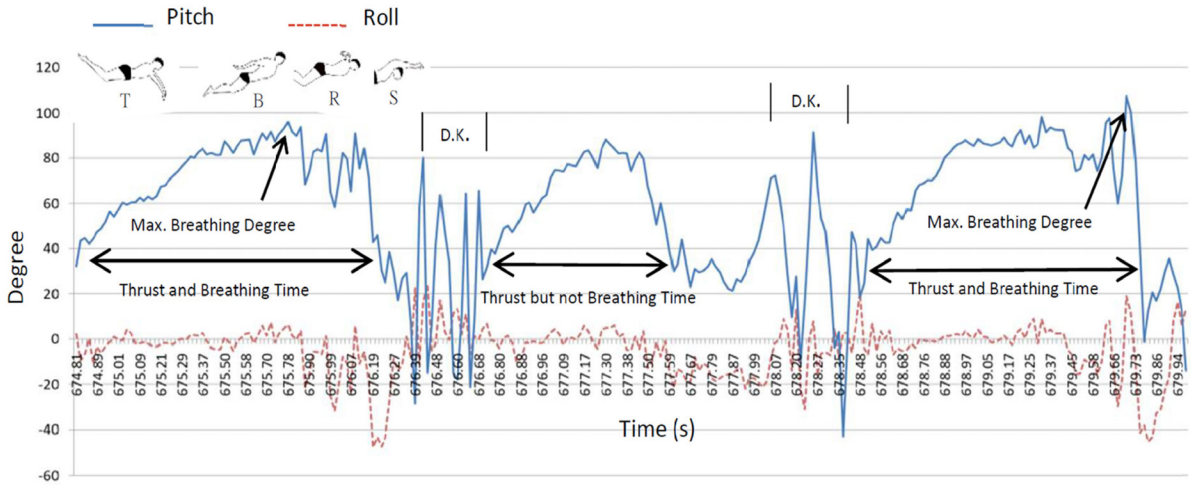

Fig. 6. Angle changes and corresponding butterfly stroke stages between 674.81 seconds and 679.94 seconds in Fig. 5

The initial analysis above shows that an IMU can effectively record the duration of a breathing motion and the maximum angles that occur during a breathing motion. It was found that breathing motions take more time than non-breathing motions. The breathing time and the maximum angles during breathing may be associated with the time it takes to complete each lap. Fig. 7 and Fig. 8 respectively represent the time it took the nine swimmers to complete the four 50m laps against their average breathing time and their average maximum breathing angle. The dotted lines in Fig. 7 and Fig. 8 respectively show the regression lines of lap time (y-axis) on average breathing time (x-axis on Fig. 7) and average maximum breathing degree (x-axis on Fig. 8) for all the swimmers. The average maximum breathing degree is denoted as "average breathing degree" in the short form. In Fig. 7, the correlation coefficient between average breathing time and lap time is $r = 0.266$ ($df = 35$, $p = 0.119$), and thus the nonsignificant low correlation coefficient represents poor prediction quality of the total regression line. Analogously to Fig. 7, as shown in Fig. 8, the correlation coefficient between average breathing degree and lap time is $r = 0.205$ ($df = 35$, $p = 0.230$), and thus the nonsignificant low correlation coefficient also represents poor prediction quality of the total regression line.

However, the between-person slopes of the regression lines for each swimmer differed significantly. Based on past research into the factors that influence swimming efficiency [9, 24], the between-person variation was related to the within-person variables of the swimmers, including age, gender, and BMI. Thus, swimming performance or the completion time of a single lap is not simply affected by the number of experiments and average maximum breathing angle but also by the physiology of the swimmers. To analyze the nature of nested relationships between within- and between- person variation, the hierarchical linear model is often used [25-26]. Therefore, a two-level regression model is applied in this study. Level 1 corresponds to the repeated measured data obtained in the four laps of each swimmer and Level 2 corresponds to the swimmer's individual variables. Clustering the data measured at different time points against the individual variables of each swimmer, a hierarchical linear model can be employed for further analysis. Aside from providing an understanding of the direct effects of the IVs on the dependent variables, this approach can also be used to determine whether interaction effects exist among variables [27].

3.2 Application of HLM for Analysis of Interaction Effects

The linear regression technique adopted in this study was the two-level HLM. The dependent variable of Level 1 was the completion time of each lap, and the predictors, or IVs, were the following data on breathing patterns obtained from each 50m lap swum by each swimmer using the butterfly stroke: average breathing time per lap (*abt*), average maximum breathing angle per lap (*abd*), and number of breaths per lap *(nb*). Level 2 corresponds to the individual variables of the swimmers, including gender, age, height, and weight. As suggested by Sedeaud et al. [9], height and weight were combined to form a single variable BMI, where BMI equals kilograms per meter squared.

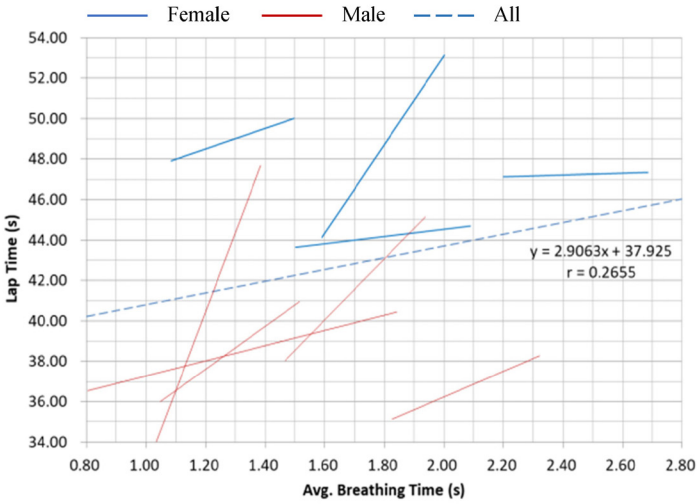

Fig. 7. Regression lines of lap time on average breathing time of individual swimmers per lap

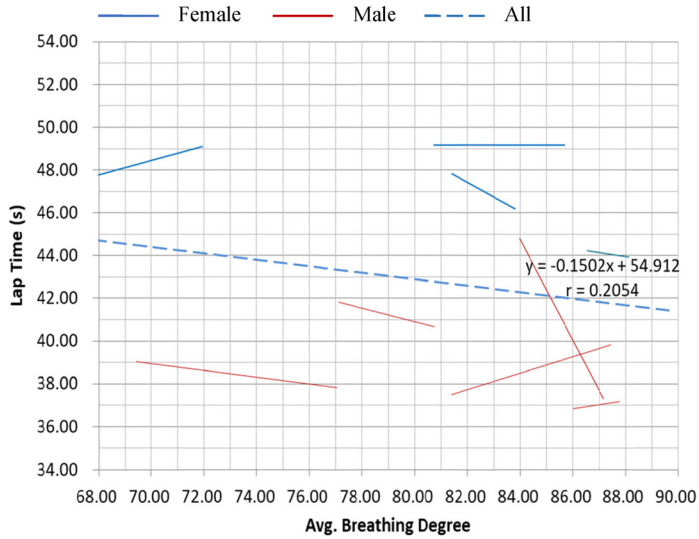

Fig. 8. Regression lines of lap time on average maximum breathing angle of individual swimmers per lap

Multicollinearity Test. During regression analysis, any high correlations (also known as multicollinearity) among the IVs will cause them to suppress one another's significance, which makes explaining the regression coefficients difficult. To eliminate IVs with multicollinearity, tolerance and the variance inflation factor (VIF) can be applied to identify multicollinearity [28]. These results are shown in Table 1. If x_i represents the dependent variable and x_1, x_2, ..., x_j represent the IVs, tolerance T_i and V_i (VIF of x_i) are defined as follows:

$$x_i = a_2 x_1 + a_2 x_2 + a_3 x_3 + \cdots + a_j x_j, i \neq j. \tag{3}$$

$$T_i = 1 - R_i^2. \tag{4}$$

$$V_i = \frac{1}{T_i}. \tag{5}$$

Table 1. Multicollinearity diagnostics of breathing patterns

IV	Tolerance	VIF
abt	.73	1.37
nb	.72	1.40
abd	.97	1.03

A greater R^2 (coefficient of determination) in Eq. (3) means that the IVs $(x_1, x_j, i \neq j)$ of the regression equation can better predict the variable x_i, which means that multicollinearity exists between x_i and the other IVs $(x_1, x_j, i \neq j)$. According to the definition in Eq. (4), the properties of T_i are the exact opposite of those of R^2: a lower T_i value indicates a greater possibility of multicollinearity, which means that a higher T_i value indicates a fainter possibility of multicollinearity. The range of R^2 is [0, 1], so the range of tolerance T_i is also [0, 1]. Thus, if tolerance T_i is greater than 0.5, the median of [0, 1], then a VIF less than 2 indicates that low multicollinearity exists among the IVs. Thus, based on Table 1, low multicollinearity exists among the 3 IVs in Level 1.

Similarly, to prevent multicollinearity, the tolerance and VIFs of the three IVs gender, age, and BMI were checked in Level 2. As shown in Table 2, all of the VIFs were less than 2, so low multicollinearity exists among the three IVs in Level 2.

Table 2. Multicollinearity diagnostics of gender, age, and BMI

IV	Tolerance	VIF
gender	.53	1.89
age	.60	1.67
BMI	.51	1.98

Interaction Effects of Age and Breathing Patterns on Lap Time. In the complete model investigating the interaction effects, *LT* denotes lap time, which is the time it took a swimmer to complete each lap using the butterfly stroke. In Level 2, *mabt* is the mean value of average breathing time of a swimmer during four laps using the butterfly stroke; *mnb* denotes the mean value of average number of breaths taken during four laps using the butterfly stroke, and *mabd* is the mean value of average maximum breathing angle of a swimmer during four laps using the butterfly stroke:

Level 1:

$$LT = \beta_0 + \beta_1(abt) + \beta_2(nb) + \beta_3(abd) + \gamma. \tag{6}$$

Level 2:

$$\beta_0 = \gamma_{00} + \gamma_{01}(age) + \gamma_{02}(mabt) + \gamma_{03}(mnb) + \gamma_{04}(mabd) + \mu_0. \tag{7}$$

$$\beta_1 = \gamma_{10} + \gamma_{11}(age). \tag{8}$$

$$\beta_2 = \gamma_{20} + \gamma_{21}(age). \tag{9}$$

$$\beta_3 = \gamma_{30} + \gamma_{31}(age). \tag{10}$$

The two-level HLM can be rewritten as the following mixed model:

$$\begin{aligned} LT = {} & \gamma_{00} + \gamma_{01}(age) + \gamma_{02}(mabt) + \gamma_{03}(mnb) + \gamma_{04}(mabd) + \gamma_{10}(abt) + \gamma_{11}(age * abt) + \\ & \gamma_{20}(nb) + \gamma_{21}(age * nb) + \gamma_{30}(abd) + \gamma_{31}(age * abd) + \mu_0 + \gamma. \end{aligned} \tag{11}$$

In Eq. (11), coefficients γ_{11}, γ_{21}, and γ_{31} determine whether age interacts with breathing patterns to influence lap time. The HLM analysis results are shown in Table 3, where γ_{11} reaches the level of significance, meaning that significant interaction effects exist between age and the average breathing time per lap. The variance of μ_0 is also significant, thereby indicating significant differences in the lap times of different swimmers.

Table 3. Mixed Model 1: Analysis of interaction effects of age and breathing patterns on lap time

Fixed Effect	γ	t	p	significance
γ_{00}	430.80	1.55	0.20	
γ_{01}	-18.57	-1.45	0.22	
γ_{02}	-1.32	-0.23	0.83	
γ_{03}	1.65	1.71	0.16	
γ_{04}	-0.21	-0.59	0.58	
γ_{10}	-64.31	-1.67	0.11	
γ_{20}	-4.24	-1.08	0.29	
γ_{30}	-2.62	-0.82	0.42	
γ_{11}	3.45	1.85	0.08	*
γ_{21}	0.19	1.06	0.30	
γ_{31}	0.12	0.81	0.43	
Random Effect	Variance	x^2	p	
μ_0	22.72	169.21	0.00	***
γ	2.05			

*$p < 0.10$. **$p < 0.05$. ***$p < 0.01$.

To illustrate the significant interaction effects of age and average breathing time per lap on lap time, the average age of the swimmers 21.13, rounded to 21, is proposed to be a cut-off value to divide the swimmers into two age groups: those older than 21 and those younger than 21. Fig. 9 represents the regression lines of lap time on average breathing time for the two age groups. As can be seen, the slopes of both regression lines are positive, which means that longer breathing time resulted in longer lap time and thus poorer swimming efficiency. However, the slopes of the two regression lines are different. The older group presents a steeper slope than the younger group. This means that the impact of breathing time on swimming performance is greater in the older group than in the younger group. Based on the slopes of the two regression lines, every increase of 1 second in the average breathing time of a swimmer in the older group per lap results in an increase of 21.057 seconds in the completion time of each lap. In comparison, every increase of 1 second in the average breathing time of a swimmer in the younger group per lap results in an increase of 7.669 seconds in the completion time of each lap.

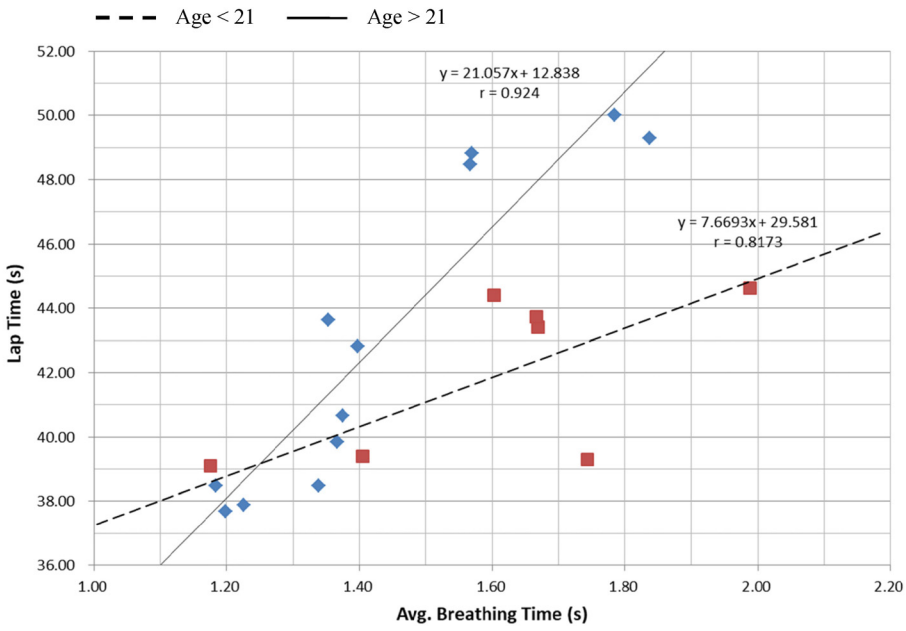

Fig. 9. Interaction effects of age and average breathing time per lap on lap time

Although average breathing time exerts a positive and significant impact on lap time in the simple regression model in Fig. 7 and Fig. 8, taking the interaction effects between age and average breathing time into account reveals that the statistically significant influence of average breathing time on swimming performance varies with the age of the swimmer.

Interaction Effects of Gender and Breathing Patterns on Lap Time. Similarly to Mixed Model 1, Eq. (11), the mixed model of the interaction effects of gender and breathing patterns on lap time is shown in Eq. (12):

$$\begin{aligned} LT = {} & \gamma_{00} + \gamma_{01}(gender) + \gamma_{02}(mabt) + \gamma_{03}(mnb) + \gamma_{04}(mabd) + \\ & \gamma_{10}(abt) + \gamma_{11}(gender * abt) + \gamma_{20}(nb) + \gamma_{21}(gender * nb) + \\ & \gamma_{30}(gender * abd) + \gamma_{31}(age * abd) + \mu_0 + \gamma. \end{aligned} \quad \textbf{(12)}$$

HLM analysis produces the coefficients in Table 4, where γ_{01} presents significant differences. This means that significant gender differences exist in lap time; γ_{10} presents positive and significant differences, indicating that a longer average breathing time results in longer lap time and thus poorer swimming performance; γ_{21} reaches the level of significance, indicating that significant interaction effects exist between gender and number of breaths per lap; γ_{31} reaches the level of significance, indicating that significant interaction effects exist between gender and average breathing time per lap. The variance of μ_0 is also significant, thereby indicating significant differences in the lap time of different swimmers.

Table 4. Mixed Model 2: Analysis of interaction effects of gender and breathing patterns on lap time

Fixed Effect	γ	t	p	significance
γ_{00}	22.32	0.95	0.40	
γ_{01}	38.87	2.21	0.09	*
γ_{02}	-4.51	-0.98	0.38	
γ_{03}	0.58	0.82	0.46	
γ_{04}	0.05	0.23	0.83	
γ_{10}	6.93	2.32	0.03	**
γ_{20}	0.52	1.70	0.10	
γ_{30}	0.06	0.43	0.67	
γ_{11}	0.38	0.12	0.91	
γ_{21}	-0.81	-2.31	0.03	**
γ_{31}	-0.47	-2.32	0.03	**
Random Effect	Variance	x^2	p	
μ_0	10.19	91.28	0.00	***
γ	1.61			

*p < 0.10. **p < 0.05. ***p< 0.01.

Gender moderates the influence of the number of breaths taken per lap on lap time. In other words, interaction effects exist between gender and the number of breaths taken, which in turn influence lap time. Fig. 10 represents the regression lines of lap time on the number of breaths per lap for the two gender groups. As can be seen, the impact of number of breaths on lap time are greater in the female swimmer group than in the male swimmer group. The slopes of the regression lines of the two gender groups are both positive. A closer look at the slopes reveal that for every additional breath taken by a female swimmer per lap using the butterfly stroke, her lap time increased by 0.522 seconds, whereas for every additional breath taken by a male swimmer per lap using the butterfly stroke, his lap time increased by 0.019 seconds.

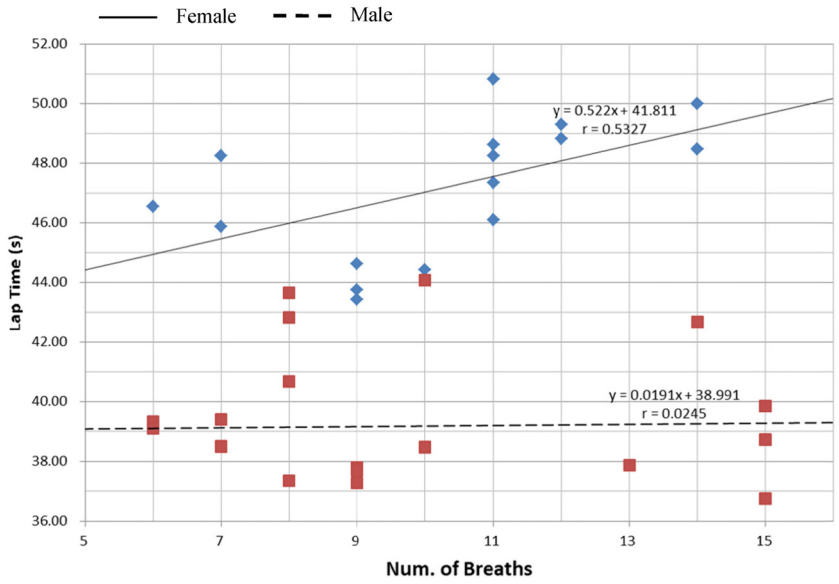

Fig. 10. Interaction effects of gender and number of breaths taken per lap on lap time

Gender also moderates influence of average maximum breathing angle on lap time. In other words, interaction effects exist between gender and average maximum breathing angle, which in turn influence lap time. As shown in Fig. 11, the slopes of the regression lines of lap time on average maximum breathing angle for the two genders were negative. A closer look at the slopes reveals that for every additional degree in the average maximum breathing angle of a female swimmer per lap using the butterfly stroke, her lap time decreases by 0.115 seconds, whereas for every additional degree in the average maximum breathing angle of a male swimmer per lap using the butterfly stroke, his lap time decreases by only 0.077 seconds. When the average maximum breathing angle per lap increases, the lap times of the female swimmers decrease by much more than those of the male swimmers.

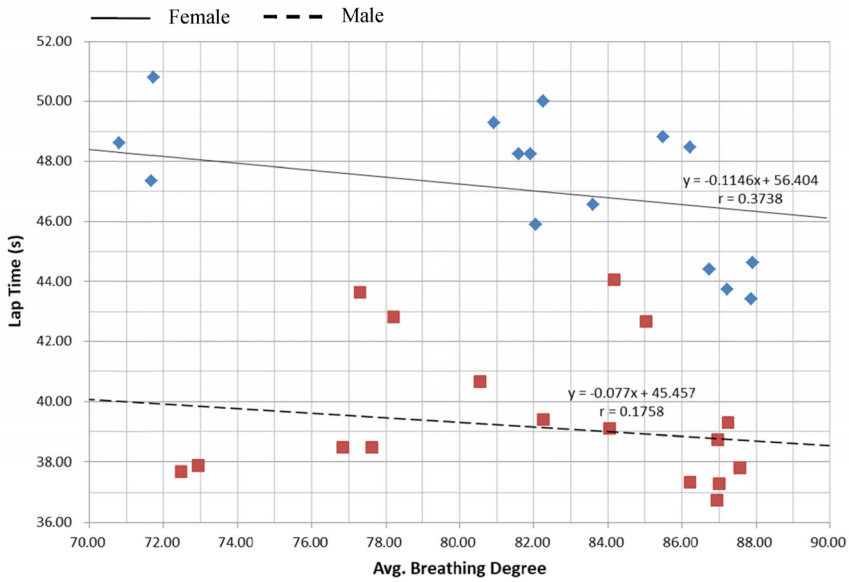

Fig. 11. Influence of interaction effects between gender and average maximum breathing angle per lap on lap time

Based on the simple regression models displayed in Fig. 7 and Fig. 8, average maximum breathing angle and the number of breaths taken per lap are not significantly correlated to lap time. However, once the interaction effects between gender and average maximum breathing angle and between gender and the number of breaths taken per lap are taken into account, gender differences in the influence of average maximum breathing angle and the number of breaths taken per lap on swimming performance can be

found. From here, it can be seen that a simple regression analysis may easily misinterpret the influence of IVs on dependent variables. Analyzing the interaction effects among predictors may reveal that the IVs produce different effects on the dependent variables in different scenarios.

Interaction Effects of BMI and Breathing Patterns on Lap Time. The mixed model of the interaction effects of BMI and breathing patterns on lap time is as shown in Eq. (13):

$$\begin{aligned} LT = {} & \gamma_{00} + \gamma_{01}(BMI) + \gamma_{02}(mabt) + \gamma_{03}(mnb) + \gamma_{04}(mabd) + \\ & \gamma_{10}(abt) + \gamma_{11}(BMI * abt) + \gamma_{20}(nb) + \gamma_{21}(BMI * nb) + \\ & \gamma_{30}(abd) + \gamma_{31}(BMI * abd) + \mu_0 + \gamma. \end{aligned} \quad \textbf{(13)}$$

HLM analysis produced the coefficients in Table 5, which γ_{01} presents significant differences and a negative relationship. This means that swimmers with greater BMI tend to have shorter lap times and thus greater swimming performance; γ_{20} presents positive and significant differences, which means that more breaths taken resulted in longer lap time and thus poorer swimming performance; γ_{30} presents positive and significant differences, which means that a greater breathing angle resulted in longer lap time and thus poorer swimming performance; γ_{21} reached the level of significance, which means that significant interaction effects exist between BMI and the number of breaths taken; γ_{31} reaches the level of significance, which means that significant interaction effects exist between BMI and average breathing time per lap. The variance of μ_0 is also significant, thereby indicating significant differences in the lap times of different swimmers.

Table 5. Mixed Model 3: Analysis of interaction effects between BMI and breathing patterns

Fixed Effect	γ	t	p	significance
γ_{00}	-242.08	-2.63	0.06	*
γ_{01}	-11.78	3.35	0.04	**
γ_{02}	3.30	0.28	0.79	
γ_{03}	1.72	1.22	0.29	
γ_{04}	-0.02	-0.06	0.95	
γ_{10}	11.97	1.00	0.33	
γ_{20}	3.67	3.19	0.00	***
γ_{30}	2.48	2.75	0.01	**
γ_{11}	-0.23	-0.47	0.65	
γ_{21}	-0.16	-3.28	0.00	***
γ_{31}	-0.17	-2.88	0.01	**
Random Effect	Variance	x^2	p	
μ_0	34.70	437.94	0.00	***
γ	1.25			

*$p < 0.10$. **$p < 0.05$. ***$p < 0.01$.

The average BMI of the swimmers was 22.79, which is rounded to 23 and used to divide the swimmers into two groups: those with a BMI greater than 23 and those with a BMI less than 23. Fig. 12 represents the regression lines of lap time on the number of breaths per lap for the two BMI groups. As can be seen, the slopes of both regression lines are different from previous conditions: one is positive, but the other is negative. For the swimmers with a lower BMI, the slope of their regression line is positive, meaning that the number of breaths taken has a positive influence on lap time; for every additional breath taken by a swimmer per lap using the butterfly stroke, his or her lap time increases by 1.253 seconds. In other words, more breaths taken means poorer swimming efficiency. In contrast, the slope of the regression line for the swimmers with a higher BMI is negative, meaning that the number of breaths taken has a negative influence on lap time; for every additional breath taken by a swimmer per lap using the butterfly stroke, his or her lap time decreases by 0.162 seconds. The influence of the number of breaths taken on lap time presents opposite trends depending on the BMI of the swimmer.

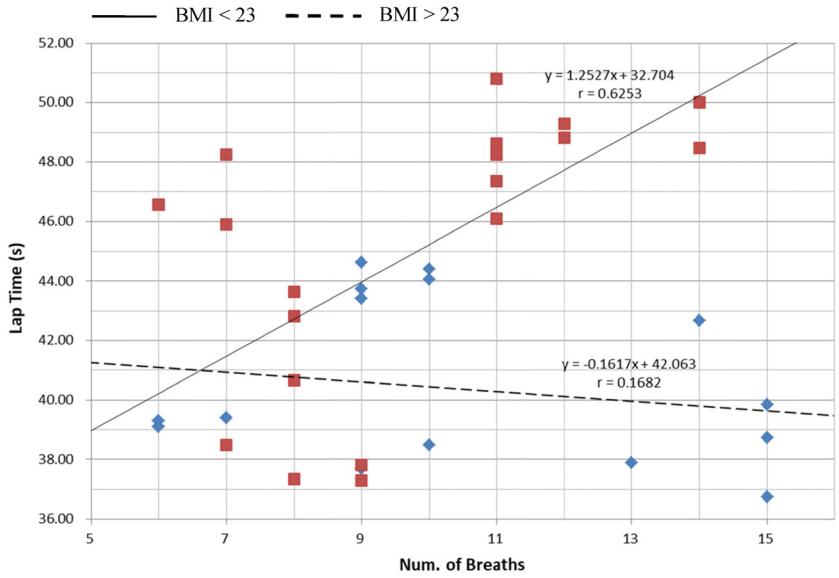

Fig. 12. Interaction effects of BMI and number of breaths taken per lap on lap time

The BMI also moderates the influence of average maximum breathing angle on lap time. In other words, interaction effects exist between BMI and average maximum breathing angle, which in turn influence lap time. In Fig. 13, one of the slopes of the regression lines for the two BMI groups is positive, and the other is negative. Thus, the influence of breathing angle on lap time may be completely different depending on the BMI of the swimmer. A closer look at the slopes reveals that for swimmers with a higher BMI, a greater average maximum breathing angle would result in longer lap time and thus poorer swimming efficiency. For every additional degree in the breathing angle of a swimmer with a higher BMI, his or her lap time increases by 0.225 seconds. In contrast, for every additional degree in the breathing angle of a swimmer with a lower BMI, his or her lap time decreases by 0.308 seconds, which means better swimming performance.

In this section, it is again found that in a simple regression analysis, average maximum breathing angle and the number of breaths taken per lap are not predictive of lap time. However, once the interaction effects between BMI and average maximum breathing angle and between BMI and the number of breaths taken per lap are taken into account, differences are found in average maximum breathing angle and the number of breaths taken per lap on swimming performance among swimmers with different BMI values.

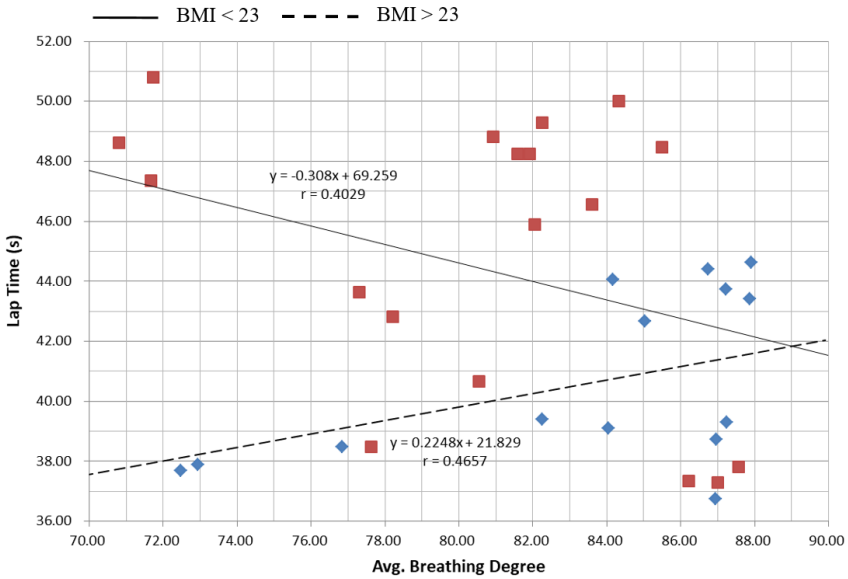

Fig. 13. Interaction effects of BMI and average maximum breathing angle per lap on lap time

4 Discussion

In this section, the features of the proposed IMU are first outlined. Then the interaction effects of age, gender, and BMI and breathing patterns on swimming efficiency are discussed.

4.1 Technical Comparison with Related Works

The present study differs from related works in two areas: complexity of collecting swimming data and the openness of hardware and software development environments for researchers. Most studies involving the butterfly stroke use expensive, difficult-to-install cameras and experimental environments to analyze swimming motions. Thus, compared to studies that used multiple cameras above and under water to analyze swimming posture [7-8, 15], the equipment developed in this study is inexpensive and easy to construct. Because of the relative complexity of analyzing the butterfly stroke, some studies even adopted humanoids to acquire research data [2, 6, 29]. Nakashima and Tsai [29] used a swimming humanoid robot to simulate the motions of the butterfly stroke and investigate the relationship between a complete motion cycle completed by a swimmer and swimming performance. Of course, the experiment in Nakashima and Tsai's study was not conducted in a normal swimming environment, either. The IMU developed in this study can be directly installed on the swimmer, and no humanoid robot is needed to simulate the motions. Thus, compared to conventional experimental scenarios, the analysis using IMUs can be conducted in a normal swimming environment, and therefore better reflects the actual posture and performance of the swimmer.

In recent studies that also used IMUs for swimming posture analysis, Staniak et al. [4] mounted a commercial IMU on the dorsal part of the pelvic girdle to analyze the coordination of butterfly stroke motions. This IMU measured 65mm×50mm×30mm, and it weighed 150 grams, making it both larger and heavier than the IMU developed in this study. They therefore had to design an elastic belt to fix and mount the IMU on the swimmer, rendering it less convenient than the one developed in this study.

Félix et al. [30] and Morouco et al. [31] employed self-developed IMUs. Their IMUs were mounted on the swimmer's lower back to analyze the balance and roll angle of the swimmer's torso and the symmetry of the swimmer's motions during four types of swimming strokes. Compared to the IMU proposed in this study, they are quite similar in purpose and function. Their results indicated that their IMUs can help prevent injury caused by motion asymmetry during swimming training and also provide reference for swimming performance improvement. Their IMUs measured 53mm×29mm×5mm, and they weighed 15 grams. Once a waterproof case was added, the dimensions and weight increased to 110mm×105mm× 8.5mm and 55 grams, respectively. Although their devices were smaller and lighter than the one developed in this study, once the waterproof case was added, they became much larger and heavier. However, the two studies conducted by Félix et al. and Morouco et al. did not provide the specifications of the MCU, accelerometer, data storage module, and battery used in their IMUs or explain how long the endurance of their IMUs was, thereby preventing other researchers from replicating them and verifying their performance. Furthermore, they claimed to use open-source firmware, but the GitHub link they provided in their papers is no longer available on the repository. The swimming posture and angle calculation algorithms are thus unknown, and the hardware module that they used was a Bitalino product rather than readily available open-source hardware.

In contrast, compared to other methods using commercial software and hardware [16-18, 20, 30-31], the open-source hardware used in this study consists of readily available and inexpensive electronic modules. The software development environment was Arduino IDE, which is an open-source and easy-to-use tool. All of the above is further supported by easy-to-obtain comprehensive documents for software and hardware resources as well as an online community. The IMU developed in this study is also rechargeable and can be used for long periods of time, and the firmware is easy to implement and modify. The completed device can be mounted on the head to analyze breathing motions, and the calculations of the angle parameters in the firmware are provided. Moreover, the swimming posture data can be easily obtained in CSV format so that researchers can analyze data easily. Thus, any interested researchers may easily replicate the software and hardware and apply them to swimming research. On the whole, the open-source software and hardware, the suitable dimensions of the product, and feasibility of empirical research and verification all make the IMU developed in this study superior to closed-source or commercial IMUs.

4.2 Interaction Effects of Age and Breathing Patterns on Swimming Performance

Using the proposed IMU, statistically significant interaction effects between swimmer age and breathing time during the butterfly stroke were found. Overall, longer breathing time means slower swimming speed. However, the influence of breathing time on lap time is greater in swimmers over 21 years old than in swimmers under 21 years old. It is speculated that this may be because younger athletes have better anaerobic work capacity than older athletes [32] and can display better efficiency during the anaerobic thrust phase of the butterfly stroke and are thus less affected by breathing time.

4.3 Interaction Effects of Gender and Breathing Patterns on Swimming Performance

Significant interaction effects exist between gender and the number of breaths taken per lap (Fig. 10) and between gender and the average maximum breathing angle (Fig. 11). In Fig. 10, the slope of the regression line of lap time on the number of breaths taken for male swimmers swimming 50 m using the butterfly stroke is slight, thereby indicating that the number of breaths taken does not significantly affect the swimming efficiency of male swimmers. In contrast, a positive correlation exists between the number of breaths taken and lap time for female swimmers. This means that when female swimmers took more breaths, their lap times tended to become longer. It is speculated that this is because male athletes have better muscle power than female athletes when it comes to short-distance races. They have greater aerobic capacity and thus better anaerobic work capacity. Short-distance swimming performance has much to do with muscle power, but not so much to do with the number of breaths taken. However, the maximum oxygen consumption (VO2max) of female athletes is lower than that of male athletes [33], so they must take more breaths to replenish the oxygen in their body. Their muscle power cannot make up for the loss in speed when they take a breath during the thrust phase, and consequently, their swimming efficiency declines.

Gender also interacts with breathing angle. In Fig. 11, the slopes of the regression lines of lap time on breathing angle for both female and male swimmers are negative, which means that a greater breathing angle results in shorter lap time. However, the impact of breathing angle on lap time is greater among female swimmers than among male swimmers, which means that significant interaction effects exist. This may be because swimming speed at the moment female swimmers complete the underwater thrust motions is not as fast as that of male swimmers because their muscle power is not as strong. As a result, a greater breathing angle can make up for the smaller bow waves and smaller breathing space created by the water flow during the butterfly stroke when speed is insufficient. It is also speculated that this may also be due to the training quality of the participants in this study. Future studies could expand the scope of the sample to obtain more accurate results.

4.4 Interaction Effects of BMI and Breathing Patterns on Swimming Performance

The 50m laps in this study represent short-distance swimming, and the butterfly stroke is a stroke that requires the greatest muscle power. In Fig. 12 and Fig. 13, the swimmers with a higher BMI swam faster than those with a lower BMI, which is similar to the results derived by Sedeaud et al [9]. However, using the proposed IMU, it is further found that significant interaction effects exist between BMI and the number of breaths taken and between BMI and breathing angle. In Fig. 12, a weak correlation exists between the number of breaths taken and lap time for swimmers with a higher BMI, whereas a significant and positive correlation exists between the number of breaths taken and lap time for swimmers with a lower BMI. Swimmers with a higher BMI have greater muscle power. They also consume oxygen more quickly to instantly provide the energy their muscles need, which helps them complete high-speed and short-distance races with anaerobic power in a short period of time. As a result, the number of breaths taken does not affect them as much.

However, Fig. 13 shows that for swimmers with a higher BMI, a greater breathing angle leads to slower swimming speed, but the effect is the opposite for swimmers with a lower BMI. It is speculated that this is because swimmers with a higher BMI have a larger and heavier physique [9] and that a greater breathing angle means greater drag. In contrast, swimmers with a lower BMI have a smaller physique and thus experience less drag, which makes it easier for them to lift their upper body out of the water for gliding during the breathing and recovery stage. This results in a greater instantaneous breathing angle but faster swimming speed.

5 Conclusions and Recommendations

To investigate the influence of breathing motions on swimming speed during the butterfly stroke, an IMU was developed in an open-source Arduino environment to collect swimming motion data in natural and non-experimental swimming environments. The proposed device has low installation costs and can effectively measure the head motions of swimmers as they breathe during the butterfly stroke. Using this experimental device, the interaction effects of swimmers' characteristics and breathing patterns on lap time were examined by multilevel models. It was found that the age, gender, and BMI of swimmers interact with their breathing patterns to influence swimming performance, which is something that has not been thoroughly discussed in existing research.

Because the IMU was developed in a modular fashion, circuit planning and module placement were not ideal. It is suggested that future studies design a dedicated printed circuit board (PCB) to address this issue. In addition, finding professional or semi-professional butterfly-stroke swimmers to participate in experiments was not easy; consequently the participants of this study were all sampled from a university swimming team. It is suggested that future studies recruit more participants from different backgrounds to further verify the influence of interaction effects among variables on swimming performance.

References

[1] M. Phelps, B. Bowman, K. Hoff, Personal best swimming instructional series: freestyle (Directed by J. Ilika), [DVD] Connecticut: Octagon, 2006.

[2] M. Cortesi, G. Gatta, Effect of the swimmer's head position on passive drag, Journal of Human Kinetics 49(1)(2015) 37-45.

[3] J. Couto, M. Franken, F.S. Castro, Influence of different breathing patterns on front crawl kinematics, Brazilian Journal of Kinanthropometry and Human Performance 17(1)(2015) 82-90.

[4] Z. Staniak, K. Buśko, M. Górski, A. Pastuszak, Accelerometer profile of motion of the pelvic girdle in butterfly swimming, Acta of Bioengineering and Biomechanics 20(1)(2018) 159-167.

[5] T. Gonjo, B.H. Olstad, Start and turn performances of competitive swimmers in sprint butterfly swimming, Journal of Sports Science and Medicine 19(2020) 727-734.

[6] R. Taiar, W. Bertucci, Th. Letellier, I. Benkemis, Y. Toshev, Experimental assessment of the drag coefficient during butterfly swimming in hydraulic flume, Acta of Bioengineering and Biomechanics 7(2)(2005) 97-108.

[7] M. Vaso, B. Knechtle, C.A. Rüst, T. Rosemann, R. Lepers, Age of peak swim speed and sex difference in performance in medley and freestyle swimming –a comparison between 200 m and 400 m in Swiss elite swimmers, Journal of Human Sport and Exercise 8(3)(2013) 954-965.

[8] H. Tanaka, D.R. Seals, Invited review: dynamic exercise performance in masters athletes: insight into the effects of primary human aging on physiological functional capacity, Journal of Applied Physiology 95(5)(2003) 2152-2162.

[9] A. Sedeaud, A. Marc, A. Marck, F. Dor, J. Schipman, M. Dorsey, A. Haida, G. Berthelot, J.-F. Toussaint, BMI, a performance parameter for speed improvement, PLoS ONE 9(2)(2014) e90183.

[10] D.J. Smith, S.R. Norris, J.M. Hogg, Performance evaluation of swimmers: scientific tools. Sports Medicine 32(9)(2002) 539-554.

[11] A.B. Craig, B. Termin, D.R. Pendergast, Simultaneous recordings of velocity and video during swimming, Portuguese Journal of Sport Sciences 6(2)(2006) 32-35.

[12] N. Vezos, V. Gourgoulis, N. Aggeloussis, P. Kasimatis, C. Christoforidis, G. Mavromatis, Underwater stroke kinematics during breathing and breath-holding front crawl swimming, Journal of Sports Science and Medicine 6(1)(2007) 58-62.

[13] A.J. Callaway, Measuring kinematic variables in front crawl swimming using accelerometers: A validation study, Sensors 15(5)(2015) 11363-11386.

[14] N. Davey, M. Anderson, D. James, Validation trial of an accelerometer-based sensor platform for swimming, Sports Technology 1(4-5)(2008) 202-207.

[15] A.J. Callaway, J.E. Cobb, I. Jones, A comparison of video and accelerometer based approaches applied to performance monitoring in swimming, International Journal of Sports Science and Coaching 4(1)(2009) 139-153.

[16] J. Pansiot, B. Lo, G.Z. Yang, Swimming stroke kinematic analysis with BSN, in: Proc. 2010 International Conference on Body Sensor Networks, 2010.

[17] S. Ganzevles, R. Vullings, P.J. Beek, H. Daanen, M. Truijens, Using tri-axial accelerometry in daily elite swim training practice, Sensors 17(5)(2017) 990.

[18] R. Mooney, G. Corley, A. Godfrey, L.R. Quinlan, G. ÓLaighin, Inertial sensor technology for elite swimming performance analysis: a systematic review, Sensors 16(1)(2016) 18.

[19] F. Dadashi, F. Crettenand, G.P. Millet, K. Aminian, Front-crawl instantaneous velocity estimation using a wearable inertial measurement unit, Sensors 12(10)(2012) 12927-12939.

[20] M. Cortesi, A. Giovanardi, G. Gatta, A.L. Mangia, S. Bartolomei, S. Fantozzi, Inertial sensors in swimming: detection of stroke phases through 3D wrist trajectory, Journal of Sports Science & Medicine 18(3)(2019) 438-447.

[21] L. Ródenas, Arduino sketch that returns calibration offsets for MPU6050 Version 1.1. <https://wired.chillibasket.com/2015/01/calibrating-mpu6050/>, 2020 (accessed 27.06.20).

[22] STMicroelectronics, AN4509 Application Note: Tilt Measurement Using a Low-g 3-Axis Accelerometer. <https://www.st.com/resource/en/application_note/dm00119046.pdf>, 2020 (accessed 27.06.20).

[23] S.W. Raudenbush, S. Bryk, Y.F. Cheong, R. Congdon, HLM6: Hierarchical Linear and Nonlinear Modeling, [software] Chicago: Scientific Software International, 2004.

[24] K. Ericsson, N. Charness, P. Feltovich, R. Hoffman (Eds.), The Cambridge Handbook of Expertise and Expert Performance (Cambridge Handbooks in Psychology), Cambridge University Press, Cambridge, 2006.

[25] J. Verner-Filion, R.J. Vallerand, A longitudinal examination of elite youth soccer players: The role of passion and basic need satisfaction in athletes' optimal functioning, Psychology of Sport & Exercise 39(2018) 20-28.

[26] W. Massey, M. Stellino, J. Geldhof, An observational study of recess quality and physical activity in urban primary schools, BMC Public Health 20(1)(2020) 792.

[27] V. Huta, When to use hierarchical linear modeling, The Quantitative Methods for Psychology 10(1)(2014) 13-28.

[28] J. Miles, M. Shevlin, Applying Regression and Correlation: A Guide for Students and Researchers, Sage, London, 2001.

[29] M. Nakashima, C.-L. Tsai, Realization and swimming performance of the butterfly stroke by a swimming humanoid robot, Journal of Aero Aqua Bio-mechanisms 6(1)(2017) 9-15.

[30] E.R. Félix, H.P. Silva, B.H. Olstad, J. Cabri, P.L. Correia, SwimBIT: A Novel Approach to Stroke Analysis During Swim Training Based on Attitude and Heading Reference System (AHRS), Sports 7(11)(2019) 238.

[31] P. Morouço, J. Pinto, E. Félix, P.L. Correia, H.P. Silva, Development of a low-cost IMU for swimmers' evaluation, in: Proc. 2020 International Conference of Biomechanics in Sports, 2020.

[32] P. Reaburn, B.J. Dascombe, Anaerobic performance in masters athletes, European Review of Aging and Physical Activity 6(1)(2009) 39-53.

[33] G. Gonzalez-Parra, R. Mora, B. Hoeger, Maximal oxygen consumption in national elite triathletes that train in high altitude, Journal of Human Sport and Exercise 8(2)(2013) 342-349.